AIAA 94-0244

An Experimental and Numerical Investigation of Drop Formation by Vortical Flows in Microgravity

L.P. Bernal; P. Maksimovic
Department of Aerospace Engineering

F. Tounsi; G. Tryggvason
Department of Mechanical Engineering and Applied Mechanics

University of Michigan
Ann Arbor, MI. 48109

32nd Aerospace Sciences Meeting & Exhibit
January 10-13, 1994 / Reno, NV

An Experimental and Numerical Investigation of Drop Formation by Vortical Flows in Microgravity

L.P. Bernal *, P. Maksimovic †, F. Toinsi £, G. Tryggvason ¥

University of Michigan

Ann Arbor, MI. 48109

Abstract

The interaction of a vortex ring with the interface between two immiscible liquids is investigated experimentally and numerically. When the Froude and the Weber numbers are high, the vortex ring penetrates the interface and forms a drop. For high Reynolds number, the evolution is relatively insensitive to the Reynolds number. The formation of the drop is examined in detail and it is shown that the drop forms by pinch off near the interface for weak rings. Multiple drops are formed for stronger rings. We use the numerical simulations to determine the boundaries for drop formation in the Fr-We plane. A rebound vortex of opposite circulation is also formed during the interaction which propagates away from the interface. Experiments and numerical results are in good agreement.

Introduction

The dynamics of fluid interfaces and free surfaces is of particular importance in microgravity where the usual domination of gravity is absent. Since surface tension forces are usually relatively weak, once the length scales are sufficiently large, the interface can undergo large deformation in response to a relatively minor disturbance. The static shape of an interface and a free surface in microgravity has been investigated by a number of researchers but the dynamic response has been studied primarily in the context of oscillating drops and other cases where the fluid motion is relatively simple. For real applications it is likely that, in general, the fluid motion will not be simple and that interface deformations due to unsteady turbulent flow may be of major importance. It is also possible that unsteady vortical fluid motion may be used to control the shape of the interface to some degree.

The dynamics of fluid interfaces and free surfaces is also important in many technological problems. Atomization of liquid fuels is strongly influenced by the interfacial properties of the fuel as well as by fluid motion within the liquid. For example, several investigators have found important effects of liquid turbulence on the spray characteristics of a nozzle.[1-3] The flow processes in typical atomization systems are very difficult to investigate experimentally because of the small size of the droplets. As we will show below the limit of interests here is high Weber and Froude number, the same as in microgravity.

In this paper we examine a simple case, the head on collision of a vortex with an initially flat fluid interface. We consider the interface between liquids of similar density to obtain a high Froude number. A better understanding of this problem should provide valuable insight on microgravity fluid mechanics and atomization processes as well.

The collision of vortex rings and pairs with a fluid interface and free surfaces has been studied by a number of investigators. One of the earliest such study was done by Linden[4] who observed large mixing due to the collision. His relatively primitive visualization technique did not, however, allow a detailed examination of the mechanisms responsible for this behavior. Dahm, Scheil, and Tryggvason[5] reexamined this problem both experimentally and numerically for a slightly miscible liquids where there were no surface tension effects at the interface. The visualization was done using a Laser Induced Fluorescence technique and the computations were done with an inviscid vortex method. The results showed that weak rings did not penetrate the interface, as expected, but instead of expanding outward, as an inviscid ring colliding with a full slip wall would do, the rings generally rebounded when a part of the interface, containing baroclinic vorticity of opposite sign to the primary vortex was torn front the interface. For rings that penetrated the interface, the fluid carried with the vortex was continuously stripped away and ejected back into the fluid where it originally came from. Thus, the ring never separated from the interface but gradually became smaller and smaller.

The collision of vortex rings and pairs with a free surface have also received considerable attention recently due to interests in the surface signature of ship wakes. Vortex rings and vortex pairs are the simplest problems which contains the basic elements of the interaction process. Sarpkaya[6] experimented with a pair of vortex filaments generated by a triangular wing and identified the key surface signature of weak pairs. This experiment was later repeated by Hirsa and Willmarth[7] who investigated the effect of surface contamination. Head on collision of vortex rings with a free surface were examined by

* Associate Professor, Department of Aerospace Engineering. Member AIAA.

† Research Assistant, Department of Aerospace Engineering.

£ Research Assistant, Department of Mechanical Engineering and Applied Mechanics.

¥ Associate Professor, Department of Mechanical Engineering and Applied Mechanics.

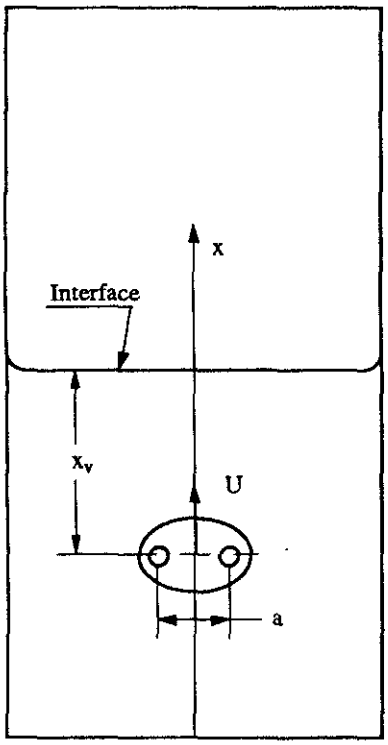

Figure 1. Schematic diagram of the flow configuration.

Kwon[8] and Kachman[9]. Bernal and coworkers[10, 11] investigated the oblique collision of rings were the ring reconnects with the free surface and forms U-vortices with its legs terminating at the surface. *Inviscid computations of a two-dimensional vortex pair* rising to the surface have been done by a number of authors, staring with Telste[12] and Yu and Tryggvason.[13] Comparison between axisymmetric simulations and experiments has been presented by Song, Bernal and Tryggvason.[14] Full viscous simulations of a vortex pair were done by Ohring and Lugth[15] who examined the depression formed outboard of weak rings (observed by Sarpkaya) and followed the evolution of a stronger pair until it had caused relatively large deformation at the free surface Tryggvason et al[16] investigated the effect of contaminants on the collision of very weak vortices where the surface could be assumed to remain flat.

While considerable work has been done on this problem, it is mostly in the parameter range that is of little interest to microgravity situations. The focus of the free surface work has been on low Froude number cases where the interface remains relatively flat, and the investigations of Linden[4] and Dahm et al[5] used miscible fluids where there are no surface tension effects. In microgravity we expect large interface deformations and we expect surface tension to be the primary restoring force. The focus of this paper is to examine the high Froude number range *where gravity effects are small, for immiscible fluids.*

Problem Statement and Techniques

The physical problem and the computational domain is sketched in Figure 1. Initially, a vortex ring of diameter a is generated in the bottom fluid about 6 cm from the interface. The ring moves to the interface with constant speed U and collides with it. If the ring is strong enough it deforms the interface and

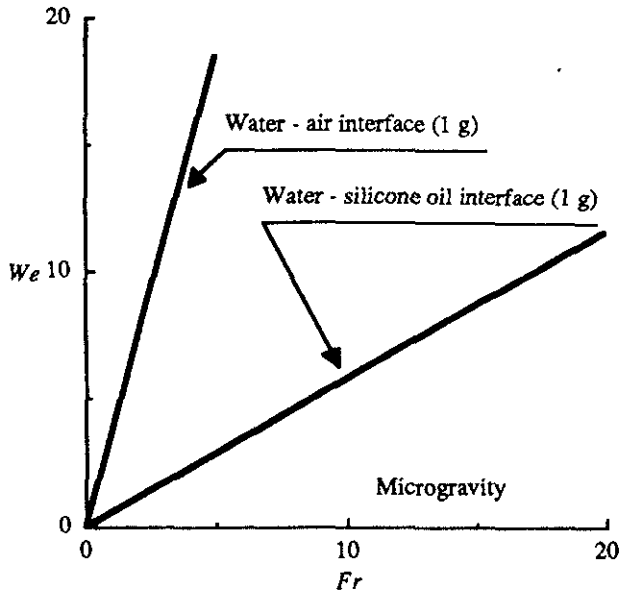

Figure 2. Plot of the Weber number vs the Froude number for typical interfaces on earth based systems (1 g) and in microgravity.

can move into the upper fluid, carrying with it a blob of the bottom fluid.

Generally, the collision and the subsequent evolution of the drop depends on fluid inertia, viscosity and surface tension. To fully specify the problem we therefore need a Weber, a Froude and a Reynolds number. These are defined by:

$$We = \frac{U}{\sqrt{\frac{\sigma}{\rho_1 a}}},$$

$$Fr = \frac{U}{\sqrt{\frac{\rho_1 - \rho_2}{\rho_1} g a}},$$

$$Re = \frac{\rho_1 U a}{\mu_1},$$

respectively. In addition, the density ratio $r = \rho_2 / \rho_1$ and the viscosity ratio $\lambda = \mu_2 / \mu_1$ must be specified. Here, the subscript 1 denotes the fluid below the interface and in the drop and 2 the fluid above the interface. Generally, we find that the results depend only weakly on Re, once it is high enough. We note that in these experiments the vortices are generated in the lower fluid and propagate upward into the lighter fluid. In the limit of small density ratios, where the Boussinesq approximation is valid, this is identical to case where the vortex would be generated in the upper fluid and propagates downward (as in the experiments of Dahm et al[5]).

In considering the effects of changing flow parameter for this problem it is important to focus on the We-Fr plane shown in Figure 2. For a fix vortex ring diameter and liquid pair, all possible vortex ring strengths (i.e. velocity U) define a straight line as shown in the Figure 2. The slope of the line is given by

$$\frac{We}{Fr} = \sqrt{\frac{\rho_1 - \rho_2}{\sigma} g a}.$$

In a microgravity environment g is very small and consequently the slope will also be small. Thus, to simulate a microgravity environment for fixed values of a and σ requires very liquid pairs of closely matched density. Another interesting case is atomization of liquid fuels. In that case a is very small and consequently we arrive at the same limit in the We-Fr plane as in microgravity.

Experimental technique

The experiments were conducted in a container $115 \times 115 \times 300$ mm. As discussed above, it is desirable to minimize the density change across the interface to simulate microgravity conditions. Several immiscible fluid pairs were tested including: water-air, water-vegetable oil and water-silicone oil. These fluid combinations had large density across the interface. For the present experiments the liquids used were a mixture of water and methanol with density 0.953 gr/cm^3 and silicon oil (Dow Corning 200, 10cs) with density 0.945 gr/cm^3. The density and viscosity ratio for this fluid system are:

$$\frac{\rho_2}{\rho_1} = 0.99, \qquad \frac{\mu_2}{\mu_1} = 5.3.$$

The interfacial tension was measured using the capillary rise technique.[17] The measured value of the interfacial tension for this system is 23.5±0.2 dynes/cm. This is significantly lower than the value for the water-silicone oil which we also measured and found in good agreement with values reported in the literature. This two fluid system was used in all the experiments reported here.

A piston-type vortex ring generator was used in the experiments. The vortex ring is produced by the motion of a piston inside a cylinder installed at the bottom of the container. The piston diameter is 12.7 mm and the length of the cylinder 12.7 mm. At the end of the stroke the piston surface is flush with the bottom of the container resulting in a smooth flat surface during the test. The piston is driven by a pneumatic actuator. The input air pressure to the pneumatic actuator determines the speed of the piston and consequently the circulation of the vortex ring. A pressure regulator and a solenoid valve were used to control the input air pressure and the initiation of the fluid motion, respectively.

To visualize the flow, a fluorescent dye (fluorescein ≈3 ppm) was added to the fluid in the vortex ring generator. The flow field was illuminated with a thin sheet of light derived from an Argon-Ion laser. The light sheet was positioned along the axis of symmetry of the flow. The fluid motion was recorded using a 35 mm SLR camera and a video system. Measurements of the position of the vortex ring and of the deformation of the interface were obtained using the video images.

Numerical Method

The computations were done with a Finite Difference/ Front Tracking method developed by Unverdi and Tryggvason.[18] The method has been discussed in detail by Unverdi and Tryggvason.[18-19] Here we only outline briefly the procedure. The actual code is an axisymmetric version written by Y.-J. Jan and discussed in Jan and Tryggvason.[20]

To solve the Navier Stokes equations we use a fixed, regular, staggered grid and discretize the momentum equations using a conservative, second order centered difference scheme for the spatial variables and an explicit second order time integration method. The pressure equation, which is non-separable due to the difference in density between the drop and the ambient fluid, is solved by a multigrid iteration. The novel aspect of the method is how the boundary between the two fluids are tracked. The interface is represented by separate computational points that are moved by interpolating their velocity from the grid. These points are connected to form a front that is used to keep the density and viscosity stratification sharp and to calculate surface tension forces. At each time step information must be passed between the front and the stationary grid. This is done by a variant on a method that is discussed in reference 18, that spreads the density jump to the grid points next to the front and generates a smooth density field that changes from one density to the other over two to three grid spaces. While this replaces the sharp interface by a slightly smoother grid interface, all numerical diffusion is eliminated since the grid-field is reconstructed at each step. The surface tension forces are computed from the geometry of the interface and distributed to the grid in the same manner as the density jump. Generally, the interface deforms greatly in our simulations and it is necessary to add and delete computational elements during the course of the calculations. When the vortices penetrate through the original interface, the fluid drop carried with the vortex is connected to the original fluid by a thin filament. Surface tension leads to a "pinch-off" where this filaments collapses. When this happens we model rupture by changing the topology of the fluid interface and removing the collapsed filament. This allows a separate drop to form. We have experimented with the detailed timing of this "rupturing" and generally found the evolution to be insensitive to the exact rupture time, as long as the filament is fully collapsed before the rupture.

The method and the code has been tested in various ways, such as by extensive grid refinement studies, comparison with other published work and analytical solutions. It has also been used to investigate a number of other multifluid problems. In addition to the computations of head-on collisions of drops by Nobari, Jan and Tryggvason,[21] Ervin[22] investigated the lift of deformable bubbles rising in a shear flow, Jan and Tryggvason[20] examined the effect of contaminants on the rise of buoyant bubbles and Nobari and Tryggvason[23] followed the coalescence of drops of different sizes. Nas and Tryggvason[24] presented simulation of thermal migration of many two dimensional bubbles.

Results and Discussions

Figure 3 shows the collision of a relatively weak ring with the fluid interface. In the top row we show photographs of the experimental results are shown, in the middle row the computed interface and the velocity field are plotted, and in the bottom row the computed vorticity field is shown. In this case the computations and experiments are for the same value of Reynolds, Froude and Weber numbers and for the same value of the density and viscosity ratios. There are however differences

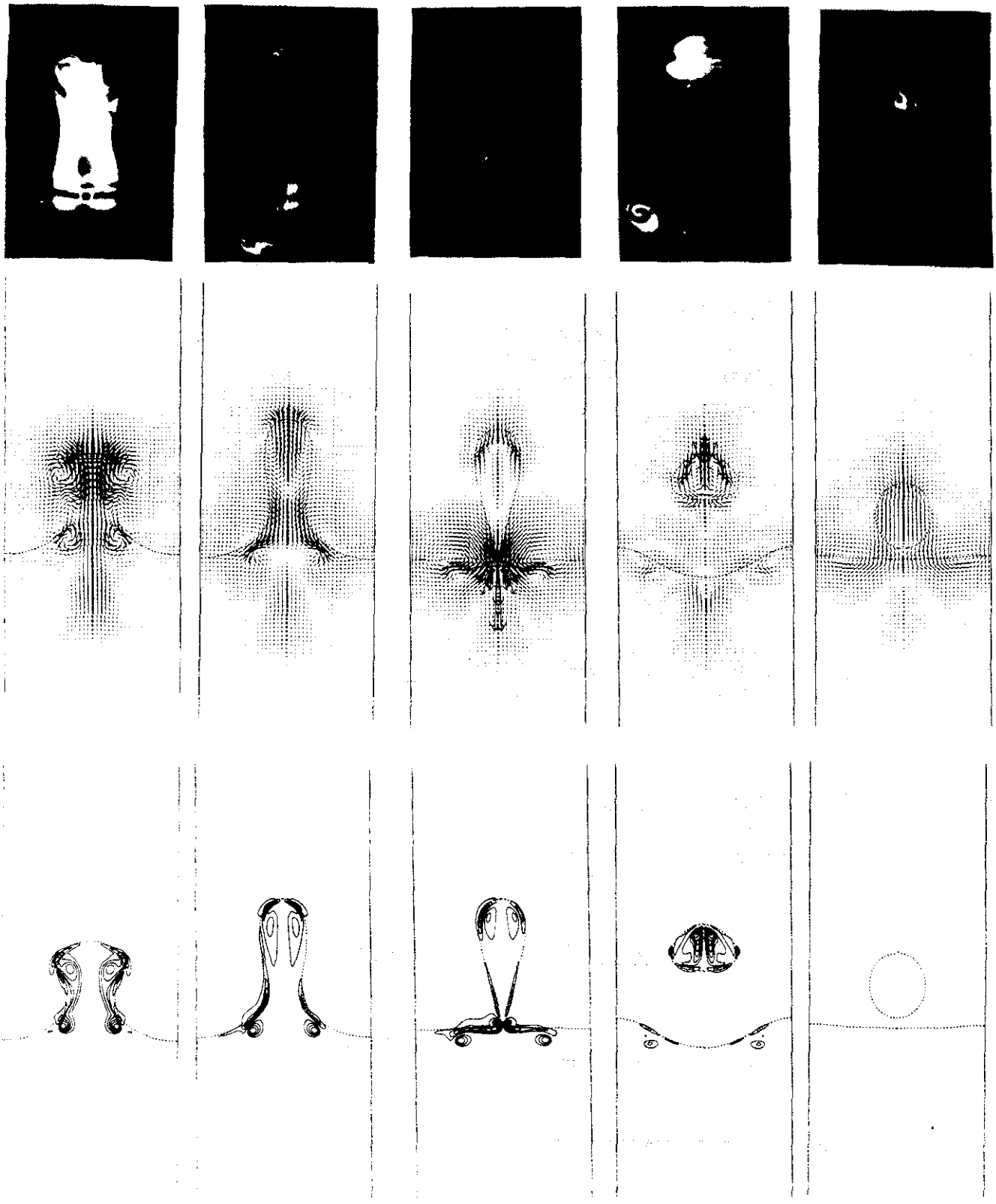

Figure 3. Interaction of a vortex ring with a fluid interface at Fr = 3.96, We = 2.45 and Re = 640. First row - flow pictures obtained at U t / a = 8.71, 11.22, 12.77 13.83, 21.37 (from left to right). Second and third row - Computational results obtained at U t / a = 3.48, 5.12, 6.46, 7.16, 10.94 (from left to right). Second row - velocity vector plot and interface elevation. Third Row - vorticity contours.

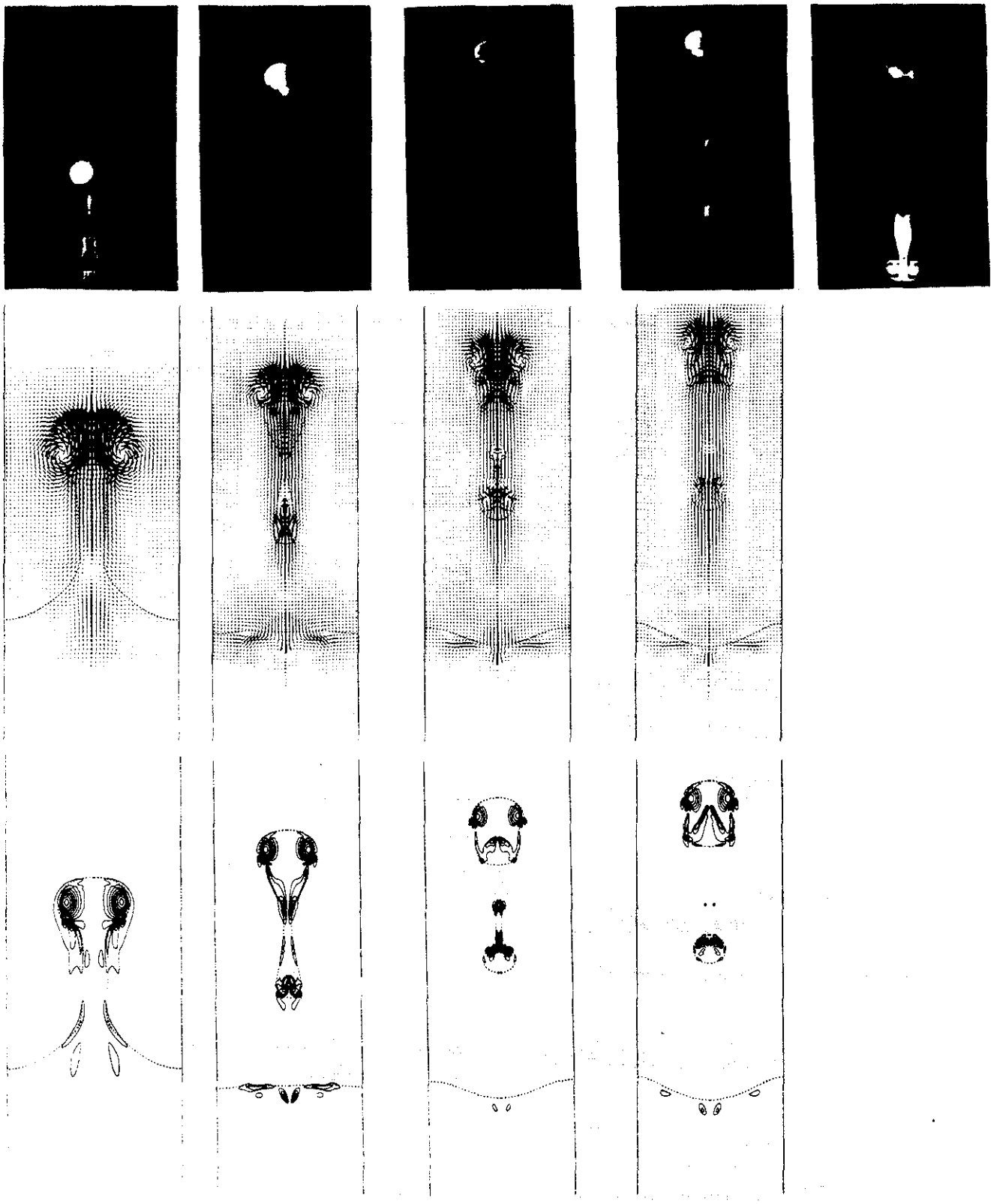

Figure 4. Interaction of a vortex ring with a fluid interface at Fr = 7.93, We = 4.68 and Re = 1,200. First row - flow pictures obtained at U t / a = 7.10, 10.34, 11.88, 12.35, 16.66 (from left to right). Second and third row - Computational results obtained at U t / a = 6.26, 9.22, 10.3, 11.48 (from left to right). Second row - velocity vector plot and interface elevation. Third Row - vorticity contours.

in the size of the computational box, the initial vorticity distribution and the initial location of the vortex. The computed shape of the interface is in good agreement with the flow visualization results. Also, the dye patterns observed in the photographs are consistent with the vorticity distributions obtained in the numerical simulations. Together they provide a detailed description of the drop formation process. As the vortex ring propagates through the interface it forms an elongated tube of lower fluid. The vorticity distribution within the vortex ring becomes elongated with some vorticity being deposited along the interface on the tube. The "pinch-off" occurs at the lower part of the tube. As the pinch-off develops there is very strong vorticity generated at neck. The computations shown that at some conditions this vorticity results in the formation a vortex ring propagating downwards in the lower fluid.

The interaction for a stronger vortex is shown in Figure 4. In this figure the flow visualization pictures are shown with the results of computations at the same conditions as indicated. In this case the vortex ring penetrates the interface and forms a thin filament of lower fluid. There are relatively small amounts of vorticity in the filament. The photographs and numerical simulations show that the thickness of the filament is not uniform. The thicker parts of the filament are associated with regions of higher level of vorticity. In this case the first "pinch-off" occurs on the lower part of the filament. However, the filament breaks also at two other places resulting in the formation of two satellite drops. These features are well captured by the numerical simulations. The last experimental condition could not be obtained in the simulations because the drop reach the upper boundary of the computational box.

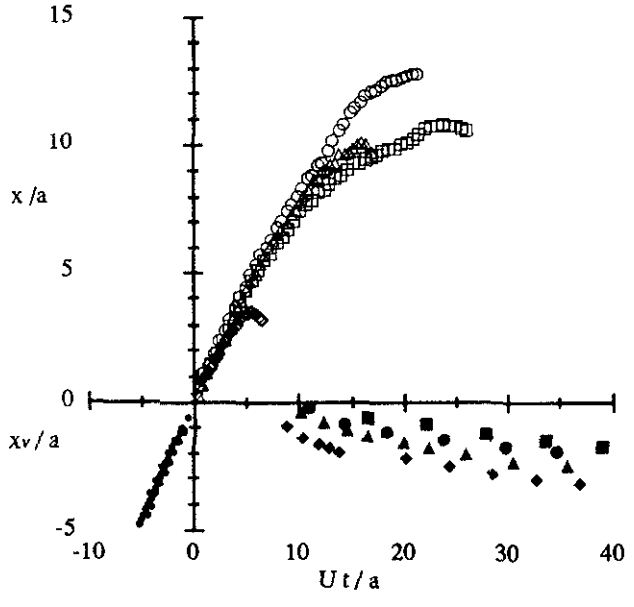

Figure 5. x-t plot of the vortex ring location and interface elevation. ◇ , Fr = 3.96 We = 2.45; Δ ,Fr = 7.93 We = 4.68; O ,Fr = 9.24 We = 5.48; □ ,Fr = 10.88 We = 6.27. Open symbols surface elevation. Solid symbols rebound vortex position.

An interesting feature of the interaction is the formation of a vortex ring in the lower fluid with circulation opposite to the circulation of the initial vortex ring. This "rebound vortex" ring propagates downward away from the interface. The rebound vortex is observed in the lower part of the last photograph in Figures 3 and 4. The numerical simulation suggest that the rebound vortex might be generated during the "pinch-off" process. However for these cases the vorticity generated during pinch-off dissipates very quickly.

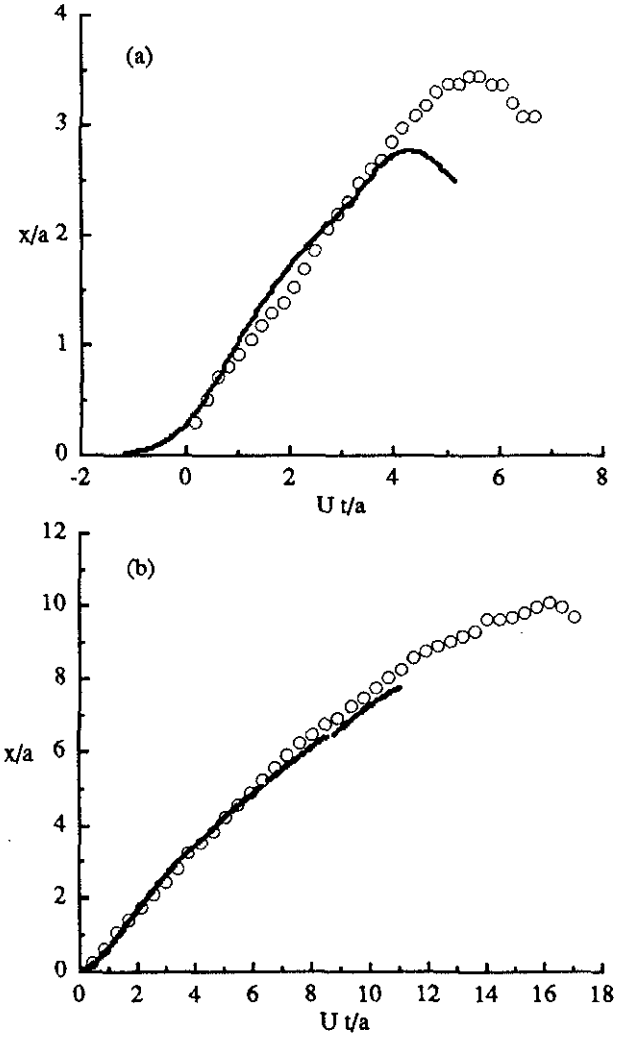

Figure 6 Comparison of numerical results (solid line) and experiments (open symbols) for the time evolution of the surface elevation. (a) Fr = 3.96 We = 2.45; (b) Fr = 7.93 We 4.68.

To examine these effects in more detail we plot in Figure 5 the position of the incoming vortex ring, the rebound vortex ring and the elevation of the interface as a function of time. All distances are measured with respect to the initial position of the interface. Negative values indicate a position below the interface. The time origin is defined as the time when the incoming vortex would have crossed the interface. The data for the initial vortex ring show excellent collapse on a straight line of slope unity as expected for the normalization used. The interface elevation is defined as the maximum elevation of the interface at

any given time. The results show an increased initial slope of the surface elevation with increase strength of the vortex ring. This indicates that stronger vortices experience less relative energy loss as they propagate through the interface. Another interesting feature is the maximum elevation reached by the interface. As the drop of heavier fluid moves upward in the lighter fluid it gradually looses kinetic energy until it stops. The maximum penetration shows an unexpected behavior. For moderate strength of the vortex ring the maximum penetration increase with the strength of the vortex ring. But at the highest Froude number tested we found a reduction of the maximum elevation. Examination of the video images shows that in this case the drop is highly deformed and has pronounced shaped oscillations. These results indicates that at high Froude/Weber number there is an increase drag of the drop as it moves through the upper fluid medium. This deformation may lead to secondary breakup of the type observed in atomization system at high Weber number

These data provide also some insight on the evolution of the rebound vortex. In all cases tested a rebound vortex was observed. It forms late in the process at a non dimensional time of approximately 10 and persists for very long times (U t / a > 80). The speed of propagation is low compared to the speed of the incoming vortex ring suggesting a fairly weak vortex. The data shows that the strength of the rebound vortex is reduced as the strength of the initial vortex is increased.

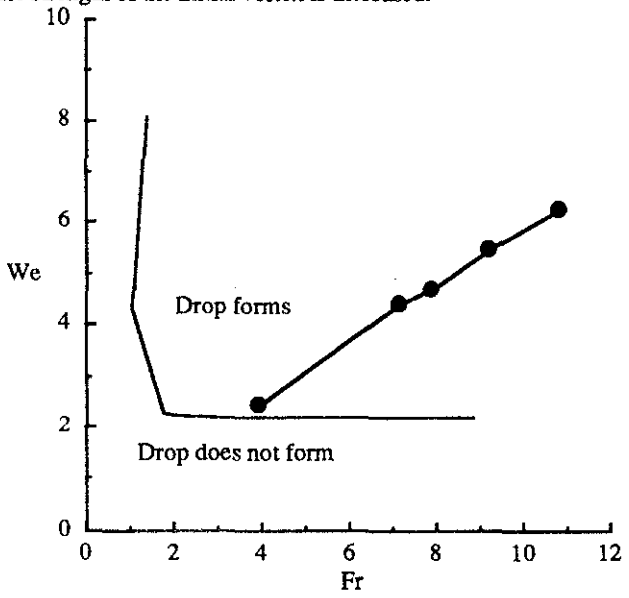

Figure 7. Drop formation boundary. The solid line are the results of computations at $\lambda = 1$ and Re = 400. Symbols are the experimental results.

A detailed comparison of the surface elevation measurements with the numerical result is shown in Figure 6. For the low strength number case the calculated values agree well with the measurement. However there is a significant discrepancy on the maximum elevation. We believe that this discrepancy is due to the different initial vorticity distribution. For the stronger vortex ring the agreement is excellent.

An important parameter of the interaction is the drop formation boundary in the Weber number - Froude number plane. Figure 7 is a plot of the computational results viscosity ratio of 1 and a Reynolds number of 400. Also plotted in the Figure 5 are experimental data for $\lambda = 0.53$. The agreement is excellent. An interesting observation is that the boundary is essentially horizontal for Froude number greater that ≈ 2. This suggests that in the high Froude number limit a minimum value of the Weber number (≈ 2) must be reached for drop formation.

Conclusion

The purpose of this paper is to examine the collision of a vortex ring with a density interface for high Froude numbers and finite Weber numbers. In these limits the vortex ring penetrates the interface easily and can form a drop of one fluid inside the other. The evolution differs here from what was observed by Dahm et al[5] for vortices colliding with a miscible fluid interface in a fundamental way. Here, we observe the formation of a distinct drop due to the action of surface tension.

The break up process is complicated and involves the formation of filament which then breaks at one or more points. The location of the breakup is in the lower part of the filament at low Weber/Froude number. With stronger initial vortex ring the beak up occurs at various points along the filament which appear correlated to the distribution of vorticity in the filament.

A rebound vortex ring is formed during the interaction. The computations indicate that the vorticity of opposite sign is introduced as the interface collapses in the final stages of the break up process.

There is in general good agreement between the computations and the experiments. A better agreement could be expected with larger computational box and with a better understanding of the effects of the initial vorticity distribution in the vortex ring

References

1. R.D. Reitz and F.V. Bracco. Mechanism of atomization of a liquid jet. Phys. Fluids, vol 25 (1982), pp1730-1742.

2 G.A. Ruff, L.P. Bernal, and G.M. Faeth, "Structure of the near-injector region of non-evaporating pressure-atomized sprays," *Journal of Propulsion and Power*,vol. 7, no. 2, pp 221-230, March-April 1991.

3 G.A. Ruff, P.-K. Wu, L.P. Bernal, and G.M. Faeth, "Continuous- and Dispersed-Phase Structure of Dense Non-Evaporating Pressure-Atomized Sprays," *Journal of Propulsion and Power*, vol. 8, no. 2, pp 280-9, March-April 1992.

4. P.F. Linden. The interaction of a vortex ring with a sharp density interface. J Fluid Mech. (1973), pp 467 - 480

5. Dahm, W.J.A., Scheil, C.M. and Tryggvason, G. Dynamics of Vortex Interaction with a Density Interface. J. Fluid Mech., **205**, 1-43, (1989).

6. T. Sarpkaya and D. O. Henderson. Free surface scars and striations due to trailing vortices generated by a submerged lifting surface. AIAA paper 85-0445

7. Hirsa, A. 1990 An experimental investigation of vortex pair interaction with a clean or contaminated free surface. Ph.D. Thesis, University of Michigan.

8. Kwon, J.T. 1989 Experimental study of vortex ring interaction with a free surface. Ph.D. Thesis, University of Michigan.

9. Kachman, N.J. 1991 The interaction of a vortex ring with a contaminated free surface. Ph.D. Thesis, University of Michigan.

10. L.P. Bernal, and J.T. Kwon, "Vortex ring dynamics at a free surface," *Phys. Fluids A*, vol. 1, no. 3, pp 449-451, March 1989.

11. N.J. Kachman, E. Koshimoto, and L.P. Bernal, "Vortex ring interaction with a contaminated surface at inclined incidence," in *Dynamics of Bubbles and Vortices Near a Free Surface*, Ed: I. Sahin, G. Tryggvason and H.L. Schreyer, AMD - vol. 119, pp 45-58, ASME Applied Mechanics Division, 1991.

12 J. G. Telste. Potential flow about two counter-rotating vortices approaching a free surface. J. Fluid Mech., **201**, 283-296, (1989).

13. Yu, D. and Tryggvason, G. The Free Surface Signature of Unsteady, Two-Dimensional Vortex flows. J. Fluid Mech., **218**, 547-572, (1990).

14. Song, M., Bernal, L.P. and Tryggvason G. Head-on Collision of a Large Vortex Ring with a Free Surface. Phys. of Fluids A **4**, 1457-1466, (1992).

15. S. Ohring and H.J.Lugth. Interaction of a viscous vortex pair with a free surface. J. Fluid Mech., **227**, 47-70, (1991).

16. Tryggvason, G., Abdollahi-Alibeik, J., Willmarth, W. and Hirsa, A. Collision of a Vortex Pair with a Contaminated Free Surface. Phys. of Fluids A **4**, 1215-1229, (1992).

17. S.B. Reddy Karri and V.K. Mathur. Measurement of interfacial tension of immiscible liquids of equal density. AIChE Journal, vol 34 (1988) no 1, p155.

18. S.O. Unverdi and G. Tryggvason. A Front Tracking Method for Viscous Incompressible Flows. J. Comput. Phys., **100** (1992) 25-37.

19. S.O. Unverdi and G. Tryggvason. Multifluid flows. Physica D **60** (1992) 70-83.

20. Jan, Y.-J., and Tryggvason, G. Computational Studies of Contaminated Bubbles. Submitted to the Physics of Fluids.

21. Nobari, M.R., Jan, Y.-J., and Tryggvason, G. Head-on Collision of Drops—A Numerical Investigation. Submitted to Phys. of Fluids A

22. E.A. Ervin: *Full Numerical Simulations of Bubbles and Drops in Shear Flow*, Ph.D. Thesis, The University of Michigan, 1993.

23. Nobari, M.R. and Tryggvason, G. Coalescence of Initially Stationary Drops. Submitted to the Journal of Fluid Mechanics.

24. Nas, S. and Tryggvason.G. Computational Investigation of the Thermal Migration of Bubbles and Drops. 1993 ASME Winter Annual Meeting.